



HAL
open science

Lightweight synchronization to NB-IoT enabled LEO Satellites through Doppler prediction

Zheng Zhou, Nicola Accettura, Raoul Prévost, Pascal Berthou

► To cite this version:

Zheng Zhou, Nicola Accettura, Raoul Prévost, Pascal Berthou. Lightweight synchronization to NB-IoT enabled LEO Satellites through Doppler prediction. The 19th International Conference on Wireless and Mobile Computing, Networking and Communications (IEEE WiMob 2023), Jun 2023, Montreal, Canada. <10.1109/WiMob58348.2023.10187879>. <hal-04054470v3>

HAL Id: hal-04054470

<https://laas.hal.science/hal-04054470v3>

Submitted on 7 Jun 2024

HAL is a multi-disciplinary open access archive for the deposit and dissemination of scientific research documents, whether they are published or not. The documents may come from teaching and research institutions in France or abroad, or from public or private research centers.

L'archive ouverte pluridisciplinaire HAL, est destinée au dépôt et à la diffusion de documents scientifiques de niveau recherche, publiés ou non, émanant des établissements d'enseignement et de recherche français ou étrangers, des laboratoires publics ou privés.



HAL Authorization

Lightweight synchronization to NB-IoT enabled LEO Satellites through Doppler prediction

Zheng Zhou*, Nicola Accettura*, Raoul Prévost[†] and Pascal Berthou*

*LAAS-CNRS, Université de Toulouse, CNRS, UPS, Toulouse, France

{firstname.lastname}@laas.fr

[†]TéSA, Toulouse, France

raoul.prevost@tesa.prd.fr

Abstract—In the last decade, it has been quickly recognized that backhauling Low Power Wide Area Networks (LPWAN) through Low Earth Orbit (LEO) satellites paves the way to the development of novel applications for a truly ubiquitous Internet of Things (IoT). Among LPWAN communications technologies, Narrowband IoT (NB-IoT) does not suffer from interference by other concurrent technologies since it works on a licensed frequency spectrum. At the same time, thanks to its medium access scheme based on contention resolution and resource allocation, NB-IoT is a key enabler for the specific market slice of IoT applications requiring a good level of reliability. In the architectural configuration analyzed throughout this contribution, an NB-IoT low power User Equipment (UE) can communicate with a LEO satellite equipped with an Evolved Node B (eNB) for a time limited to the visibility window of that satellite from the UE position on the Earth. However, the Doppler effect inherent to the time-varying relative speed of the eNB needs to be dealt with additional resources. The solutions proposed until now are non-trivial, thus making the use of NB-IoT for ground-to-satellite communications still expensive and energetically inefficient. Timely, this contribution proposes a procedure for a UE to infer the future values of the Doppler shift from the beacon signals so that frequency pre-compensation can be easily applied in the following interactions during the visibility time. The presented simulation results show that a UE needs to listen to about 10 beacon signals in 1 second to accurately and robustly predict the Doppler curve, thus enabling a lightweight (and eventually truly energy-efficient) implementation of NB-IoT over ground-to-satellite links.

Index Terms—NB-IoT, LEO Satellites, Doppler effect

I. INTRODUCTION

In recent years, Low Power Wide Area Networks (LPWAN) have emerged as a critical enabling technology for the Internet of Things (IoT) since they offer a cheap and affordable solution for connecting very low-power devices over long distances [1]. As well the increasing availability of novel application scenarios has pushed each LPWAN technology to target a subset of such applications and to better their access scheme off through the conception and design of additional communication modes [2]. Among these, the Narrowband IoT (NB-IoT) [3] technology is the main solution over the licensed spectrum, fitting applications that need a higher level of reliability. It also stands out for low power consumption, capacity, and security [4]. Introduced by 3GPP starting from Release 13, NB-IoT is based on Long-Term Evolution (LTE), so it can operate within the related licensed spectrum and

utilize most of the same technologies and infrastructure, including Evolved Node B (eNB). Any eNB acts like a gateway, forwarding messages received from cheap low-power User Equipment (UE) over the radio medium through the core network. Remarkably, the high capacity and high reliability of NB-IoT depend on its resource allocation strategy, which prevents collisions when transmitting data. In turn, such a strategy relies on tight synchronization in frequency and time.

More recently, it was recognized that the large scope provided by NB-IoT and, in general, by all LPWANs is still not possible for some unreachable areas such as oceans and deserts or when there are some geographical obstacles like mountains. In that, a disruptive solution has been provided by the use of LPWAN-enabled satellites to collect IoT data over such geographical areas, thus making ground-to-satellite communications an increasingly popular solution for novel and advanced IoT applications in the context of smart agriculture, environmental monitoring, and emergency management, etc. [5]. Specifically, Low Earth Orbit (LEO) satellites provide lower latency than those in orbits with higher altitudes, and the cost of CubeSat LEO satellites has gradually decreased in the last few years [6], [7]. In addition, the high maneuverability of such satellites helps in avoiding obstructions that may affect signal strength. All these features make LPWAN-enabled LEO satellites the best solution for IoT applications in remote areas. From an architectural point of view, these satellites act as gateways by forwarding messages between IoT devices and a base station, both on the ground. In the case of NB-IoT, the role of a gateway is played by an eNB embedded in the LEO satellite. However, the use of NB-IoT for ground-to-satellite communications is not cheap and is not energy efficient because of the presence of some technical barriers hindering the worldwide adoption of the same solution. Due to the high-speed motion of LEO satellites, communications are affected by the Doppler effect, with a measured frequency offset of ± 40 kHz for satellites elevated 600 km above the ground [8]. As a result, the signal can be significantly degraded, and link layer frames can be lost. Moreover, NB-IoT transmission delays typically range from hundreds of milliseconds to almost 12 seconds [9], depending on factors like data size, network load, and link quality. During this period, the frequency shift caused by the Doppler effect may vary from tens to several kilohertz, so the Doppler frequency shift cannot be calculated

through the initial synchronization of NB-IoT. Therefore, a varying Doppler shift is the biggest challenge for the massive adoption of NB-IoT between ground UEs and eNBs mounted on LEO satellites. Similarly, if the UE cannot pre-compensate the Doppler shift, the listening frequency band of the LEO satellite will be larger and have higher power consumption. In the same way, UE should listen to a larger frequency band for the following interactions. In this sense, starting from Release 17 [10], 3GPP has been specifying how NB-IoT/eMTC (enhanced Machine Type Communication) can support non-terrestrial networking and the case scenario pictured above: each UE must be equipped with a Global Navigation Satellite System (GNSS) receiver and must be configured with the ephemeris of the satellite using the Two-Line Element set (TLE) to pre-compensate the Doppler shift and propagation delay. However, the need for a GNSS receiver implies extra power consumption and an incremented cost of UEs.

Timely, this paper makes possible the prediction of the Doppler effect by estimating the trajectory of the satellite in the sky without GNSS capabilities. This is done through the observation of NB-IoT downlink signals. The computed prediction is used to pre-compensate the Doppler shift. The related routines implemented in the firmware of any ground UE are meant to be triggered only if the synchronization signals are detected to be frequency-shifted. Otherwise, the UE works according to default terrestrial NB-IoT policies. Thus, this solution makes transparent the use of any firmware-updated UE in both terrestrial NB-IoT networks and ground-to-satellite NB-IoT links.

The feasibility of such a system over ground-to-satellite links is studied by simulating the unpredictability of the errors that may happen in estimating the Doppler curve, and the results presented hereafter encourage such an investigation. In detail, Section II presents a review of the related works, while Section III pictures the proposed idea. Then, Section IV presents the results of a simulation-based analysis. Finally, Section V draws conclusions and envisages future works.

II. RELATED WORKS

The use of NB-IoT for ground-to-satellite communications got significant interest from the research community. Some of them [11]–[13] assume that each UE is equipped with a GNSS receiver and uses the captured positioning together with the Two-Line Element set (TLE) to determine the relative position of the LEO satellite and use this information to predict the frequency and time offset. However, as said in Section I, the need for GNSS receivers plays against the two objectives of energy efficiency and cost-effectiveness.

With a different approach, [14] proposes a Doppler pre-compensation of NB-IoT beacon signals that does not require any change on the configuration of UEs: they do not need either to be equipped with GNSS or to listen to a wider spectrum to cope with Doppler effect. This strategy is energy efficient for UEs but requires significant changes to the hardware and software of the eNB-equipped satellite. In fact, from the software point of view, the eNB uses a centralized

resource allocation scheme based on the partition of the entire coverage area into multiple small regions: the differential Doppler shift is reduced on a per-region basis, thus improving the quality and reliability of the communication link. From the hardware point of view, a multi-beam satellite is required to work properly on a specific channel with each region. Finally, since the UE does not pre-compensate the frequency shift, the satellite must listen to a wider bandwidth to catch any frame arriving on a frequency shifted according to the Doppler effect. Instead, [15] proposed to modify the NB-IoT physical layer about what concerns the preamble structure and the synchronization procedure to achieve uplink synchronization. In addition, there is no pre-compensation, thus requiring the UE to keep receiving the synchronization signals until sending the first uplink signal. Both these solutions require significant changes either to the NB-IoT protocol or to the hardware.

For the sake of a clear positioning, it is worth mentioning other works not related to NB-IoT yet dealing with downlink synchronization between a ground terminal and a LEO satellite. To achieve such synchronization, the influence of the Doppler frequency shift must be eliminated. First of all, two main research lines have been identified [16]: (i) *Doppler characterization*, i.e., how to measure the Doppler shift in a received signal and determine the relative speed of the transmitter; (ii) *Doppler compensation*, i.e., how to correct the transmitting frequency to cope with the Doppler shift in a signal. In regard to Doppler characterization, the studies of [17]–[19] demonstrate that the Doppler shift can be estimated by low-power devices, thus making this approach applicable to IoT devices. Instead, with regard to Doppler compensation, a standard strategy is to use “Fast-tracking,” i.e., a terminal on the ground should keep receiving downlink beacon signals to calculate the real-time Doppler offset [8], [19]–[21]. However, this approach requires high processing units and constant communication capabilities, thus not fitting the desired behavior of low-power duty-cycled IoT devices. Instead, the “predictive tracking” strategy is to estimate the Doppler curve during the satellite’s passage from the Doppler-shifted frequency of several consecutive downlink synchronization signals. Once the Doppler curve is understood, the expected trajectory is also known, thus requiring no further estimation of the frequency shift. [22] uses the received signal combined with satellite position information from TLE to plot a Doppler curve, allowing for prediction of the Doppler shift at each moment throughout the process. Using a mathematical model, the authors of [23] proposed a method to figure out the Doppler curve through two downlink signals. However, neither of these papers considered the impact of the downlink signal measurement error on the drawing of the Doppler curve.

III. PROPOSED APPROACH

In order to gently introduce the core idea of this paper, it is first worth giving some details about how an NB-IoT communication is set up. When a UE wakes up (or it is bootstrapped), the first step is to perform a cell search to obtain key information about the network. This is done by waiting

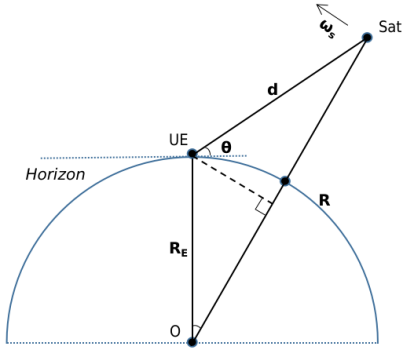


Fig. 1. LEO satellite and UE.

for a Narrowband Primary Synchronization Signal (NPSS) received from an eNB in the scope. The NPSS is a 1ms-long signal periodically broadcast by any eNB every 10 ms. Such a signal is used by the UE for the initial time and frequency synchronization [24]. Once synchronized, the UE waits for the Narrowband Second Synchronization Signal (NSSS) to obtain the cell ID. After this downlink synchronization process is finished, NB-IoT will receive network system information through other downlink messages, i.e., the Master Information Block (MIB) and System Information Block (SIB). At this point, the UE is able to send uplink messages and complete the setup of reliable bidirectional communication.

The synchronization process described so far is not directly applicable to non-terrestrial communications without some trick. A LEO satellite equipped with an eNB is responsible for forwarding messages transmitted between the UE and the ground base station. Unlike traditional NB-IoT networks, the UE needs to receive several NPSS to draw the Doppler curve and get synchronized to the network. Understanding the Doppler curve is functional for the UE to pre-compensate the frequency used to transmit (or receive) link layer frames during the visibility time of the eNB. For this reason, the next subsection describes how to link a Doppler curve with a given satellite trajectory, while Section III-B details the model used to identify a Doppler curve based on NPSS noisy receptions.

A. Doppler Curve

The Doppler effect deals with a perceived frequency shift due to the relative motion between a transmitter and a receiver. In detail, the frequency f_r observed by the receiver is

$$f_r = \left(1 + \frac{\Delta v}{c}\right) f_0 = f_0 + \Delta f, \quad (1)$$

where f_0 is a known emitted frequency used by the transmitter to propagate the signal, Δv is the relative speed between transmitter and receiver, and c is the speed of light. Finally, Δf is the Doppler frequency shift.

As explained in [23], obtaining the relative speed change between the satellite and the UE is necessary. For the sake of readability, the topological scenario used in this paper is pictured in Fig. 1. In that, R_E is the Earth radius, and R is the radius of the satellite orbit, while ω_s is the angular velocity of

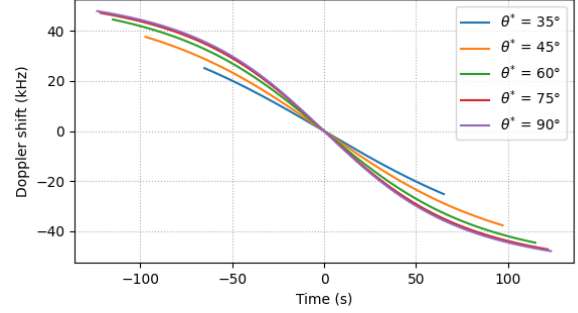


Fig. 2. Example of Doppler effect with a 600-km LEO Satellite.

the satellite. Even if ω_s varies with latitude due to the Earth's rotation, such a variation is negligible for low to medium orbit altitudes [23], so it is assumed constant hereafter.

Then, θ is the elevation angle between the horizon and the line of sight of the receiver. Due to a series of physical reasons (including the antenna, the altitude, etc.), communication can happen only if the elevation angle is bigger than a minimum value θ_{\min} . In the rest of the paper, the assumed value of θ_{\min} is 30° [25]. Furthermore, the trajectory of a LEO satellite passing through the communication scope of a UE is featured by a maximum elevation angle θ^* . In other words, for a given satellite pass, θ^* is the elevation angle achieved when the satellite is the closest to the UE. Clearly, the range of θ^* lies in the following interval $[\theta_{\min}, 90^\circ]$. When the satellite passes directly above the UE, $\theta^* = 90^\circ$. Another angle of interest is the one between R and R_E when when $\theta = \theta^*$, namely α_0 :

$$\alpha_0 = \arccos\left(\frac{R_E}{R} \cos \theta^*\right) - \theta^*. \quad (2)$$

Under [23], during a satellite pass, the origin $t = 0$ on the timeline corresponds to the instant when the elevation angle is $\theta = \theta^*$. The relative distance $d(t)$ between the UE and the satellite at a given instant t during a satellite pass is then

$$d(t) = \sqrt{R_E^2 + R^2 - 2RR_E \cos(\omega_s t) \cos(\alpha_0)}, \quad (3)$$

and the relative speed between UE and the LEO satellite is

$$\dot{d}(t) = \frac{RR_E \omega_s \sin(\omega_s t) \cos \alpha_0}{d(t)} = -\Delta v. \quad (4)$$

Combining (1) with (4) and (3), the frequency shift formulation depending on t , R , R_E , ω_s , and α_0 is

$$\Delta f = -\frac{f_0}{c} \frac{RR_E \omega_s \sin(\omega_s t) \cos(\alpha_0)}{\sqrt{R_E^2 + R^2 - 2RR_E \cos(\omega_s t) \cos(\alpha_0)}}. \quad (5)$$

Fig. 2 shows the Doppler curves related to a 600 km elevated LEO satellite with several values of θ^* . The carrier frequency used here and for the rest of the paper is 2.4 GHz.

B. Estimation of the Doppler curve

In reality, the measured Doppler shift will always be affected by an error. The assumption made throughout this

contribution is that such an error can be modeled as an Additive White Gaussian Noise (AWGN), with zero mean ($\mu = 0$) and a variance value σ^2 that can be properly tuned to mimic different noise levels. Such an assumption comes from the consideration that the Gaussian distribution well approximates randomness in many natural phenomena and engineering problems. More specifically, it is possible to relate the measured Doppler shift, $\Delta \hat{f}$, to the actual one, Δf , as

$$\Delta \hat{f} = \Delta f + \varepsilon, \quad (6)$$

where ε is the measurement error.

However, the actual Doppler shift Δf is unknown. Indeed, its formulation, given by (5), depends on the time instant t , which is unknown. According to the model presented so far, t represents the instant when a beacon NPSS signal was sent by satellite within the portion of its trajectory within the scope of the UE receiving that signal. At the same time, t can be always expressed as the sum of the unknown instant when the very first NPSS was received at the UE, t_0 , and the known interval Δt , that could be expressed as multiple of the time between 2 consecutive NPSS transmissions, i.e., 10 ms. Substituting $t = t_0 + \Delta t$ in (5), the supposed model for Δf is $D(\Delta t)$ and depends on the known independent variable Δt :

$$\begin{aligned} D(\Delta t) &= \\ &= -\frac{f_0}{c} \frac{RR_E \omega_s \sin(\omega_s(t_0 + \Delta t)) \cos(\alpha_0)}{\sqrt{R_E^2 + R^2 - 2RR_E \cos(\omega_s(t_0 + \Delta t)) \cos(\alpha_0)}} \end{aligned} \quad (7)$$

with t_0 and θ^* being unknown parameters to be determined (θ^* does not appear directly in the formulation of (7), because it is embedded within α_0).

More specifically, assuming to receive m signals, the method of least squares can be used to determine such parameters. In that, the vector of measured data is

$$\Delta \hat{\mathbf{f}} = [\Delta \hat{f}_1, \dots, \Delta \hat{f}_m], \quad (8)$$

so that the vector of the residuals, $\mathbf{r}(\beta) = [r_1, \dots, r_m]$, is composed by the following elements

$$r_i = \Delta \hat{f}_i - D(\beta; \Delta t_i) \quad \text{with } i = 1, \dots, m \quad (9)$$

where $\beta = [\theta^* \ t_0]^T$ is the vector of unknown parameters and Δt_i is the time interval between t_0 and the i -th NPSS signal. The resulting loss function

$$L(\beta) = \mathbf{r}(\beta) \cdot \mathbf{r}(\beta)^T \quad (10)$$

can be minimized through the Gauss-Newton method.

The optimal solution for the two parameters can be found by iterating the following algorithm

$$\beta_{k+1} = \beta_k - (J^T J)^{-1} J^T \mathbf{r}(\beta), \quad (11)$$

where J is the Jacobian matrix of the residual and k is the iteration number.

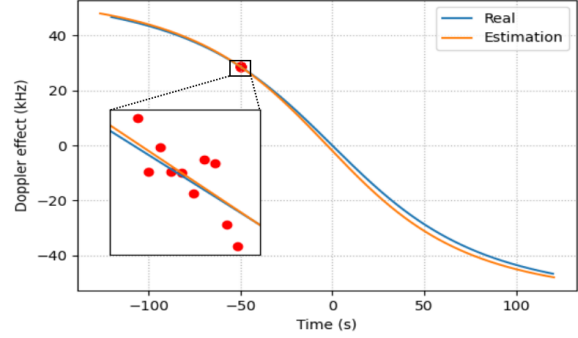


Fig. 3. Example of a sample simulation result with $\sigma = 20$.

IV. SIMULATION RESULTS

In this section, some results are presented based on the simulation of the proposed method for estimating the Doppler curve. First, each NPSS signal is generated together with the corresponding Doppler effect. Then, this value is incremented (or decremented) according to a random value drawn according to a normal distribution with zero mean and variance equal to σ^2 in order to mimic the AWGN-like measurement noise. Next, these values are meant to represent the measured NPSS signals and are used within the model in Section III-B to estimate the Doppler curve. Finally, the estimated Doppler curve is compared against the actual one to evaluate the model's performance. The index used to measure such a performance is the maximum communication time, i.e., how long the estimated Doppler curve can be used in subsequent interactions between the UE and the eNB-equipped LEO satellite to pre-compensate the transmission and reception frequencies on the UE. In detail, such a performance index is defined as the time interval during which the error between the estimated Doppler curve and the real one stays below a given threshold value. As a narrowband communication technology, NB-IoT usually has a small maximum allowed frequency error (950 Hz) [14]. To provide reliable results, a conservative approach has been adopted, and the threshold value for determining the maximum communication time was set to 500 Hz.

To help in appreciating the performance evaluation, Fig. 3 shows an example of how to interpret the simulation results. The figure compares the original Doppler curve and the estimated one calculated through the mathematical model. Herein, the standard deviation σ of the simulated AWGN-like source of errors is set to 20 Hz, and the UE needs to receive 10 NPSS beacons in order to derive the estimation of the Doppler curve. Zooming on the evaluated time interval (see Fig. 3), it can be noticed that each signal is affected by a random error, and the final fitting result is very close to the original Doppler curve, which shows that the mathematical model is feasible.

Furthermore, each point on the following plots represents an average of 3000 in simulated scenarios. Each scenario is obtained by randomly choosing the time for the first NPSS

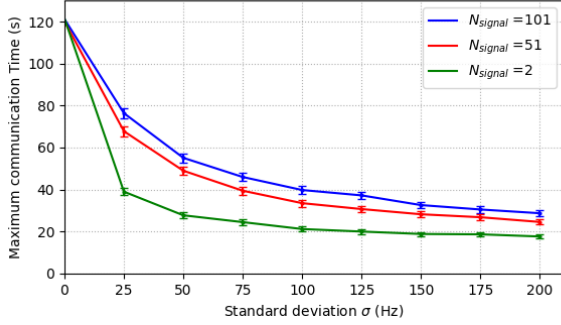


Fig. 4. Maximum communication time ($T_{\text{measure}} = 1$ s).

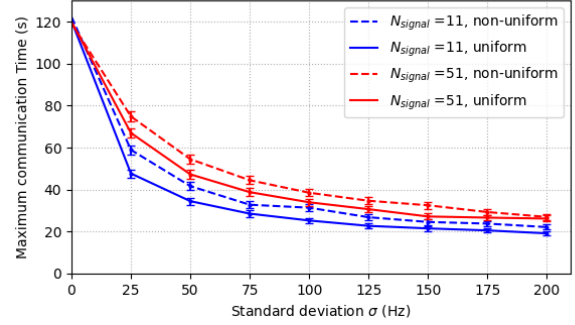


Fig. 6. Maximum communication time with different sampling strategies.

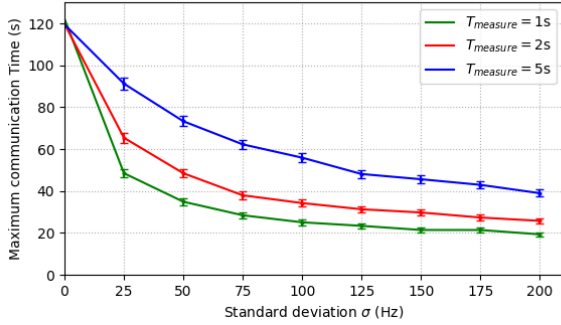


Fig. 5. Maximum communication time ($N_{\text{signals}} = 11$).

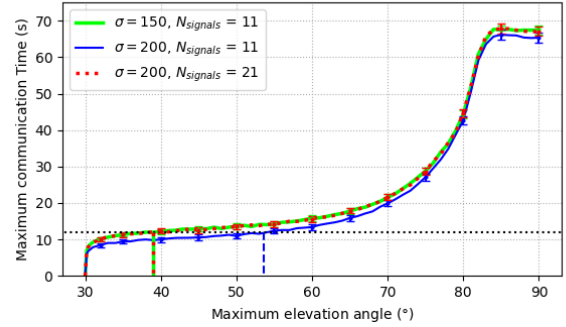


Fig. 7. Maximum communication time with different θ^* ($T_{\text{measure}} = 1$ s).

reception in the visibility time related to the chosen maximum elevation angle. 95% confidence intervals are also shown for the sake of statistical significance.

First, the impact of different amounts of NPSS used for the Doppler curve prediction was studied. The maximum elevation angle θ^* was fixed to 70° for all simulations, while the measurement time was limited to 1 second. The NPSS used for estimating the Doppler curve are taken uniformly over the measurement time. For instance, when the number of used NPSS is 51, the time interval between two consecutive NPSS used for the estimation is 20 milliseconds. As shown in Fig. 4, the prediction accuracy increases with the amount of NPSS used for predicting the Doppler curve. Yet, it also comes with a higher energy consumption. Therefore, there is a need to find a trade-off between prediction accuracy and energy efficiency.

Pushing forward the analysis, Fig. 5 plots simulation results obtained when the number of used NPSS in the Doppler curve prediction is fixed to 11, while the measurement time T_{measure} is varied among 1, 2, 5 s. The considered NPSS are taken uniformly in time over the measurement interval. Results show that the wider the intervals, the more accurate the prediction. This is because a larger measurement interval allows for a difference in Doppler shift between consecutive measurements, which is greater than the measurement error: larger measurement intervals produce more accurate predictions. However, due to the short pass time, prolonging such an interval can lead to potential interference from other causes,

which can negatively affect the accuracy of the predictions.

Another step ahead in the analysis can be done by considering a non-uniform sampling of the received NPSS. Here, the measurement time T_{measure} is set to 1 second. The non-uniform sampling strategy involves concentrated measurements at the beginning and at the end of the measurement period, resulting in uneven time intervals. For example, if 11 NPSS are used in total over a measurement time of 1 s, the first 5 considered NPSS are those transmitted at the very beginning of such interval (each of them is sent every 10 ms), while the remaining 6 NPSS are those received at the very end of the same measurement interval (each of them is also sent every 10 ms). The results related to this approach are those pictured with dashed lines in Fig. 6. Comparing the two sampling strategies, it can be seen that with the same number of used NPSS, the highest sampling frequency used in the non-uniform strategy produces a more accurate prediction for the Doppler curve, as already proved in Fig. 4.

All results presented so far show how the sampling strategy can affect the accuracy of prediction of the Doppler curve in NB-IoT communications to LEO satellites. All in all, it was found that increasing the number of received signals and using non-uniform time or larger intervals between measurements can improve the accuracy of predictions. Considering the energy consumption and limited communication time, these factors must be balanced according to the measurement error.

For the sake of generality, the impact of the maximum

elevation angle θ^* was also studied by varying it between 30° and 90° (see Fig. 7). Considering that the maximum value of the time required for an NB-IoT session must be handled in the architecture analyzed so far (i.e., 12 seconds [9], see the horizontal dotted line in Fig. 7), results show that for a noisy environment featured by $\sigma = 150$, the reception of 11 NPSS beacons within 1 second is sufficient to accommodate the communication requirements for most of the UEs in the scope of the eNB-equipped LEO satellite: if $\theta^* \geq 40^\circ$, then the NB-IoT session can happen, otherwise the UE should not start the NB-IoT session and wait for another pass (see the green line). If the noise is featured by a higher noise, i.e., $\sigma = 200$, then the UE able to handle an NB-IoT session are those having $\theta^* \geq 55^\circ$ (see the blue line). However, in the same noisy scenario, if UEs collect 21 NPSS (see the red dotted line), then they can be able to handle an NB-IoT session for $\theta^* \geq 40^\circ$, as in the case of $\sigma = 150$ and 11 NPSS collected. In other words, when the noise increases, the possibility of handling an NB-IoT session can be ensured by collecting more NPSS to predict the Doppler curve, thus trading off energy efficiency for better communication ability.

V. CONCLUSION

This paper focused on the use of LEO satellites to backhaul NB-IoT networks. It also introduced a lightweight strategy to be implemented on ground NB-IoT UEs to compute the Doppler curve based on the reception of several synchronization signals from eNB mounted on LEO satellites. Such a curve is used to predict the Doppler shift and pre-compensate the transmission and reception frequency in the following interaction during the satellite pass. Based on a simulation campaign, it was demonstrated that the proposed method effectively synchronizes the frequency of NB-IoT downlink signals for LEO satellite communication systems by utilizing the NPSS even in the presence of measurement errors. Compared with other methods, the proposed method requires a lower level of complexity and can be implemented with simple equipment on satellites and ground terminals. The simulations also show that the method can achieve high synchronization accuracy and reliability under various operating factors, making it suitable for practical use in LEO satellite communication systems. To completely show the inherent effectiveness, the proposed method will be compared against other synchronization strategies available in the literature. In addition, periodic wake-up schemes for UEs will be investigated in order to save the energy stored in the feeding batteries while preserving the accuracy of the Doppler curve estimation.

ACKNOWLEDGMENT

This work was financed in whole or in part by the IRT St. Exupéry ELLIOT project, by the French National Research Agency (ANR) under the project LabEx CIMI (grant ANR-11-LABX-0040) within the French State Program "Investissements d'Avenir," by the Stic-AmSud 21-STIC-12 STARS project, and by ANR under the STEREO project (grant ANR-22-CE25-0014-01).

REFERENCES

- [1] B. S. Chaudhari, M. Zennaro, and S. R. Borkar, "Lpwan technologies: Emerging application characteristics, requirements, and design considerations," *Future Internet*, vol. 12, 2020.
- [2] Z. Zhou, M. Afhamisis, M. R. Palattella, N. Accettura, and P. Berthou, "Pervasive LPWAN connectivity through LEO Satellites: trading off reliability, throughput, latency, and energy efficiency," in *Low-Power Wide-Area Networks: Opportunities, Challenges, Risks and Threats*, I. Butun and I. F. Akyildiz, Eds. Springer, 2022. [Online]. Available: <https://hal.laas.fr/hal-03844534>
- [3] "3GPP Specifications, Available online: <https://3gpp.org/>"
- [4] K. Mekki, E. Bajic, F. Chaxel, and F. Meyer, "A comparative study of lpwan technologies for large-scale iot deployment," *ICT Express*, vol. 5, 2019.
- [5] J. A. Fraire, S. Céspedes, and N. Accettura, "Direct-to-satellite iot - a survey of the state of the art and future research perspectives - backhauling the iot through leo satellites," in *AdHoc-Now*, 2019.
- [6] Z. Qu, G. Zhang, H. Cao, and J. Xie, "Leo satellite constellation for internet of things," *IEEE Access*, vol. 5, 2017.
- [7] A. H. Poghosyan and A. Golkar, "Cubesat evolution: Analyzing cubesat capabilities for conducting science missions," *Progress in Aerospace Sciences*, vol. 88, 2017.
- [8] W. Wang, Y. Tong, L. Li, A.-A. Lu, L. You, and X. Gao, "Near optimal timing and frequency offset estimation for 5g integrated leo satellite communication system," *IEEE Access*, vol. 7, 2019.
- [9] A. Hoglund, D. P. Van, T. Tirronen, O. Liberg, Y. Sui, and E. A. Yavuz, "3gpp release 15 early data transmission," *IEEE Communications Standards Magazine*, vol. 2, no. 2, 2018.
- [10] "3GPP Release 17th."
- [11] A. Guidotti, A. Vanelli-Coralli, M. Caus, J. Bas, G. Colavolpe, T. Foggi, S. Cioni, A. Modenini, and D. Tarchi, "Satellite-enabled lte systems in leo constellations," in *2017 IEEE International Conference on Communications Workshops (ICC Workshops)*, 2017.
- [12] M. Conti, S. Andrenacci, N. Maturo, S. Chatzinotas, and A. Vanelli-Coralli, "Doppler impact analysis for nb-iot and satellite systems integration," in *ICC*, 2020.
- [13] O. Liberg, S. E. Löwenmark, S. Euler, B. Hofström, T. Khan, X. Lin, and J. Sedin, "Narrowband internet of things for non-terrestrial networks," *IEEE Communications Standards Magazine*, vol. 4, no. 4, 2020.
- [14] O. Kodheli, S. Andrenacci, N. Maturo, S. Chatzinotas, and F. Zimmer, "Resource allocation approach for differential doppler reduction in nb-iot over leo satellite," in *ASMS/SPSC*, 2018.
- [15] H. Chougrani, S. Kisseleff, W. A. Martins, and S. Chatzinotas, "Nb-iot random access for nonterrestrial networks: Preamble detection and uplink synchronization," *IEEE IoT Journal*, vol. 9, no. 16, 2022.
- [16] B. You, H. Jung, and I.-H. Lee, "Survey on doppler characterization and compensation schemes in leo satellite communication systems," in *2022 27th Asia Pacific Conference on Communications (APCC)*, 2022.
- [17] M. Neinavaie, J. Khalife, and Z. Kassas, "Blind doppler tracking and beacon detection for opportunistic navigation with leo satellite signals," in *2021 IEEE Aerospace Conference (50100)*, 2021.
- [18] M. Pan, J. Hu, J. Yuan, J. Liu, and Y. Su, "An efficient blind doppler shift estimation and compensation method for leo satellite communications," in *IEEE ICCT*, 2020.
- [19] Z. Huang, "A pilot-aided method of doppler offset estimation and compensation," in *ICCCS*, 2021.
- [20] J. Li, Y. Zhang, Y. Zhang, W. Xiong, Y. Huang, and Z. Wang, "Fast tracking doppler compensation for ofdm-based leo satellite data transmission," in *IEEE ICC*, 2016.
- [21] C. An and H.-G. Ryu, "Compensation systems and performance comparison of the very high doppler frequency," in *IEEE ComNet*, 2020.
- [22] H. Rouzegar and M. Ghanbarisabagh, "Estimation of doppler curve for leo satellites," *Wireless Personal Communications*, 2019.
- [23] I. Ali, N. Al-Dhahir, and J. E. Hershey, "Doppler characterization for leo satellites," *IEEE Trans. Commun.*, vol. 46, 1998.
- [24] A. Shimura, M. Sawahashi, S. Nagata, and Y. Kishiyama, "Physical cell id detection performance applying frequency diversity reception to npss and nsss for nb-iot," in *APCC*, 2018.
- [25] N. Fadilah, M. A. Arifin, A. H. Qonita, N. Najati, B. Pratomo, Dwiyanto, and E. N. Nasser, "Link and doppler analysis for leo constellation space-based iot," in *IEEE ICARES*, 2022.